

# Superscaling in charged current neutrino quasielastic scattering in the relativistic impulse approximation

J.A. Caballero<sup>a</sup>, J.E. Amaro<sup>b</sup>, M.B. Barbaro<sup>c</sup>, T.W. Donnelly<sup>d</sup>, C. Maierov<sup>e</sup> and J.M. Udias<sup>f</sup>

<sup>a</sup>Departamento de Física Atómica, Molecular y Nuclear, Universidad de Sevilla, 41080 Sevilla, SPAIN

<sup>b</sup>Departamento de Física Moderna, Universidad de Granada, 18071 Granada, SPAIN

<sup>c</sup>Dipartimento di Fisica Teorica, Università di Torino and INFN,  
Sezione di Torino, Via P. Giuria 1, 10125 Torino, ITALY

<sup>d</sup>Center for Theoretical Physics, Laboratory for Nuclear Science and Department of Physics,  
Massachusetts Institute of Technology, Cambridge, MA 02139, USA

<sup>e</sup>INFN, Sezione di Catania, Via Santa Sofia 64, 95123 Catania, ITALY and

<sup>f</sup>Departamento de Física Atómica, Molecular y Nuclear,  
Universidad Complutense de Madrid, 28040 Madrid, SPAIN

Superscaling of the quasielastic cross section in charged current neutrino-nucleus reactions at energies of a few GeV is investigated within the framework of the relativistic impulse approximation. Several approaches are used to describe final state interactions and comparisons are made with the plane wave approximation. Superscaling is very successful in all cases. The scaling function obtained using a relativistic mean field for the final states shows an asymmetric shape with a long tail extending towards positive values of the scaling variable, in excellent agreement with the behavior presented by the experimental scaling function.

PACS numbers: 25.30.Pt; 13.15.+g; 24.10.Jv

In the context of inclusive quasielastic (QE) electron scattering at intermediate to high energies, the concepts of scaling [1] and superscaling [2] have been explored in previous work [3, 4], where an exhaustive analysis of the  $(e, e')$  world data demonstrated the quality of the scaling behavior. Scaling of the first kind (no dependence on the momentum transfer) is reasonably well respected at excitation energies below the QE peak, whereas scaling of second kind (no dependence on the nuclear species) is excellent in the same region. The simultaneous occurrence of both kinds of scaling is called superscaling. At energies above the QE peak both scaling of the first and, to a lesser extent, of the second kind are shown to be violated because of important contributions introduced by effects beyond the impulse approximation, namely, inelastic scattering [5] together with correlations and meson exchange currents in both the 1p-1h and 2p-2h sectors [6, 7].

The scaling analysis of  $(e, e')$  data has been exploited in [8] to predict  $(\nu, \mu)$  neutrino-nucleus cross sections. This strategy is based on the assumption that a universal scaling function exists, which is valid for both electron and neutrino scattering reactions, provided that the corresponding kinematics are similar.

In this letter we investigate the QE scaling properties of charged-current (CC) neutrino-nucleus scattering within the context of the Relativistic Impulse Approximation (RIA). After verifying that various RIA models do superscale, we compare the associated scaling functions with the  $(e, e')$  “experimental” one. This allows us to check the consistency of the above-mentioned universality assumption and the capabilities of different models in describing the dynamical properties of the nucleus which are embodied in the experimental scaling function.

Here we follow the general procedure of scaling and

superscaling studies, namely we first construct inclusive cross sections within a model and then obtain scaling functions by dividing them by the relevant single-nucleon cross sections weighted by the corresponding proton and neutron numbers [3, 4, 9]. The scaling function is plotted against the scaling variable  $\psi(q, \omega)$ , with  $q$  and  $\omega$  the momentum and energy transferred in the process, and its scaling properties analyzed.

Within the RIA framework CC neutrino-nucleus QE scattering is described by assuming that at the  $\nu-\mu$  vertex one vector boson is exchanged with the nucleus, interacting with only one nucleon, which is then emitted while the remaining (A-1) nucleons in the target remain as spectators. The nuclear current operator is thus taken to be the sum of single-nucleon currents, for which we employ the usual relativistic free nucleon expressions [8, 10]. The RIA approach has been extensively and successfully applied in investigations of exclusive electron scattering reactions [11]. Further details on the model have been presented in [10, 12, 13].

We describe the bound nucleon states as self-consistent Dirac-Hartree solutions, derived within a Relativistic Mean Field (RMF) approach using a Lagrangian containing  $\sigma$ ,  $\omega$  and  $\rho$  mesons [14]. For the description of the outgoing nucleon states we consider several different approaches. In one we use plane-wave spinors (thus no Final-State Interactions (FSI)), corresponding to the Relativistic Plane-Wave Impulse Approximation (RPWIA). However, comparisons with data require a more realistic description of the final nucleon state, which should include the effects due to FSI. This is accomplished by using distorted waves, given as solutions of a Dirac equation containing a relativistic potential, namely, the Relativistic Distorted-Wave Impulse Approximation (RDWIA).

The use of complex relativistic optical potentials has

proven to be very successful in describing exclusive (semi-inclusive)  $(e, e'p)$  scattering reactions [11]. For inclusive processes such as  $(e, e')$  and  $(\nu, \mu)$ , where a selection of the exclusive single-nucleon knockout channel cannot be made, one should not include the imaginary term of the optical potential, whose absorption represents the loss of flux into inelastic channels — these should be retained for inclusive scattering, but not for exclusive reactions, and ignoring them would lead to an underestimation of the inclusive cross section [13]. We consider two choices for the real part. The first uses the phenomenological relativistic optical potential from the energy-dependent,  $A$ -independent parameterizations derived by Clark *et al.* for  $^{12}\text{C}$  (EDAIC),  $^{16}\text{O}$  (EDAO) and  $^{40}\text{Ca}$  (EDAIa) [15], but with their imaginary parts set to zero. The second approach is by means of distorted waves obtained with the same relativistic mean field used to describe the initial bound nucleon states. We refer to these two FSI descriptions as real Relativistic Optical Potential (rROP) and Relativistic Mean Field (RMF), respectively. Note that the RMF model is constructed in a way that maintains the continuity equation.

In this work we neglect the Coulomb distortion of the outgoing lepton. Checks made within the effective momentum approximation [16] confirm that these effects are within 3-4% for all cases presented and that our general conclusions about scaling are not affected by them.

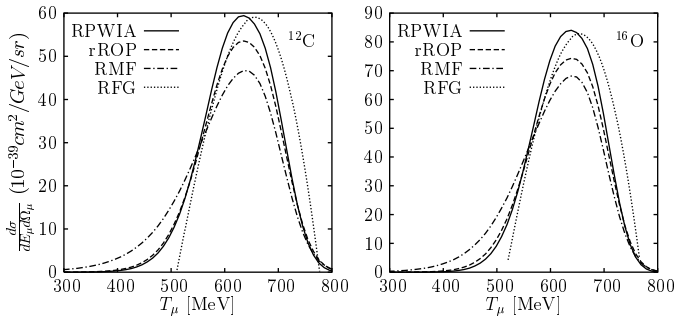


FIG. 1: Quasielastic differential cross section  $d\sigma/dE_\mu d\Omega_\mu$  versus the muon kinetic energy  $T_\mu$  for the reaction  $(\nu_\mu, \mu^-)$  on  $^{12}\text{C}$  (left) and  $^{16}\text{O}$  (right). The incident neutrino energy is  $\varepsilon_\nu = 1$  GeV and the muon scattering angle is  $\theta_\mu = 45^\circ$ . In each panel we present results for RPWIA (solid), rROP (dashed) and RMF (dot-dashed). The cross section for the RFG model is also presented for reference (dotted).

Our results for CC neutrino-nucleus QE scattering are presented in Fig. 1, where we show the differential cross section ( $d\sigma/dE_\mu d\Omega_\mu$ ) as a function of the outgoing muon kinetic energy for  $^{12}\text{C}$  and  $^{16}\text{O}$ . In each case the cross sections are shown for the three approaches to FSI: RPWIA (solid lines), rROP (dashed) and RMF (dot-dashed). For reference we also include the results obtained within the Relativistic Fermi Gas (RFG) (dotted) with Fermi momenta  $k_F = 228$  MeV/c for  $^{12}\text{C}$  [4] and  $k_F = 216$  MeV/c for  $^{16}\text{O}$  [17]. The RFG curves contain a phenomenologi-

cal energy shift [4] yielding RFG cross sections which are very similar to the RPWIA results.

The mean field dynamics in the initial and final nuclear states lead to cross sections having tails that extend both below and above the kinematical region where the RFG is defined. With FSI included we observe a significant reduction of the cross section, particularly in the case of the RMF potential where it is seen to be about 20% for both nuclei in the region close to the maximum. Notice also a very slight displacement in the maximum of the cross section in the cases of the two RIA-FSI models. However, the most striking feature is the long tail displayed by the RMF cross section for small muon kinetic energies. This corresponds to transferred energies above the QE peak, i.e., positive values of the scaling variable. These FSI effects lead to a clear asymmetry in the RMF cross section, in contrast to the RPWIA and rROP results. The discrepancy between the two FSI approaches is linked to the different energy dependence of the optical potential: for high nucleon kinetic energies (small muon energies) the magnitudes of the scalar and vector potentials involved in the rROP model are significantly reduced with respect to the RMF [11]. This explains why the rROP cross section is closer to the RPWIA case, and moreover, why the main difference between the two models is observed in the region of lower muon energies. Note that the asymmetric broadening of the RMF cross section is similar to that observed in non-relativistic models of the FSI, described by some as medium modifications of the p-h propagator [17, 18].

Let us now study the superscaling properties. We present results for the scaling function  $f(\psi')$ , which is obtained by dividing the calculated differential cross section of Fig. 1 by the single-nucleon cross section as given in Eqs. (45,52,86-94) of [8]. This function is plotted against the shifted QE scaling variable  $\psi'$  defined as

$$\psi' \equiv \frac{1}{\sqrt{\xi_F}} \frac{\lambda' - \tau'}{\sqrt{(1 + \lambda')\tau' + \kappa\sqrt{\tau'(1 + \tau')}}}, \quad (1)$$

where  $\lambda' \equiv (\omega - E_{shift})/2m_N$ ,  $\kappa \equiv q/2m_N$ ,  $\tau' \equiv \kappa^2 - \lambda'^2$ , and  $\xi_F \equiv \sqrt{1 + (k_F/m_N)^2} - 1$ . The energy shift  $E_{shift}$  has been taken from [4]. Results correspond to fixed scattering muon angle  $\theta_\mu = 45^\circ$ . Similar scaling functions are obtained with other values, and thus the following conclusions can be considered to be valid in general.

Scaling of the first kind is explored in Fig. 2, where we present  $f(\psi')$  for  $^{12}\text{C}$  at three different values of the incident energy, namely  $\varepsilon_\nu = 1, 1.5$  and  $2$  GeV. Each panel in the figure corresponds to a different description of the FSI. As one can see, the scaling function for the RPWIA and rROP models shows a very mild dependence on the momentum transfer in both positive and negative  $\psi'$  regions. In the case of the RMF, a slight shift occurs in the so-called “scaling region”  $\psi' < 0$ , whereas for  $\psi'$  positive the model breaks scaling at roughly the 30% level in the energy region explored here. This is not in con-

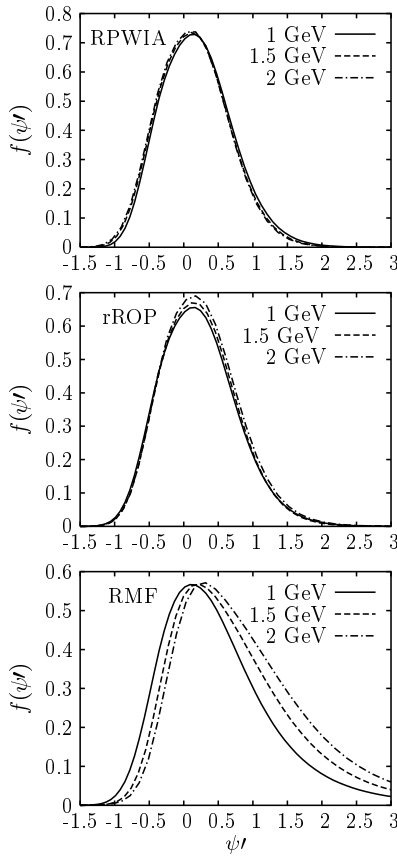


FIG. 2: Scaling function for three values of the incident neutrino energy  $\varepsilon_\nu$ . Results correspond to  $^{12}\text{C}$  and  $\theta_\mu = 45^\circ$ . Top, middle and bottom panels refer to RPWIA, rROP and RMF models (see text for details).

flict with the experimental  $(e, e')$  data that indeed leave room for some breaking of first-kind scaling in this region, due partly to  $\Delta$  production and partly to other contributions, such as MEC and their associated correlations in the 2p-2h sector [7]. It is striking that the RMF model, in spite of being based on the impulse approximation, leads to the same kind of behavior which is apparently not reproduced by uncorrelated models in the impulse approximation. Importantly, the RMF scaling function exhibits a significant asymmetry, being larger for positive  $\psi'$ , which persists for all neutrino energies (actually increasing with  $\varepsilon_\nu$ ).

Scaling of the second kind is studied in Fig. 3, where the scaling function evaluated for three nuclei,  $^{12}\text{C}$ ,  $^{16}\text{O}$  and  $^{40}\text{Ca}$ , is presented for the RPWIA (top panel), rROP (middle) and RMF (bottom) descriptions of the final states. The values of the Fermi momentum used range from  $k_F = 216$  MeV/c for  $^{16}\text{O}$  to  $k_F = 241$  MeV/c for  $^{40}\text{Ca}$  [4]. The initial bound states have been obtained using the parameters of the set NLSH [19]. Results with other parameterizations are similar and do not change the general conclusions. As observed, the differences introduced by changing nucleus are small. We may con-

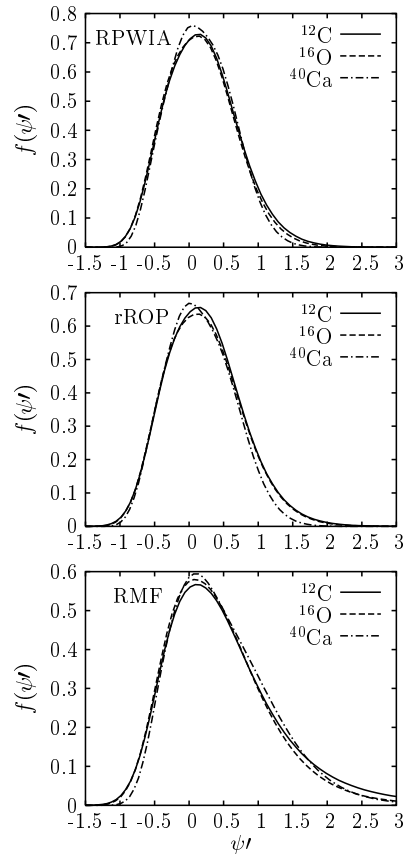


FIG. 3: Scaling function for three nuclei:  $^{12}\text{C}$ ,  $^{16}\text{O}$  and  $^{40}\text{Ca}$ . Results correspond to  $\varepsilon_\nu = 1$  GeV and  $\theta_\mu = 45^\circ$ . Top, middle and bottom panels as in previous figure.

clude that within the present model scaling of second kind is very successful. Indeed, this is just what is seen experimentally, at least for  $\psi' < 0$  where scaling of the second kind is excellent [2, 3].

Finally, in Fig. 4 we compare the “theoretical” super-scaling function corresponding to RPWIA, rROP and RMF with the averaged QE “experimental” function obtained from the analysis of  $(e, e')$  data together with a phenomenological parameterization [2, 8, 20].

First we observe the symmetric character of the RPWIA and rROP results, which clearly differ from the experimental function. On the contrary, the RMF curve displays a pronounced tail that extends toward positive values of  $\psi'$ , following closely the asymmetric behavior of the data and yielding excellent agreement with the phenomenological scaling function. The asymmetric shape of the RMF result constitutes a basic difference not only from the other two models explored in this work, but also from other modeling presented in the literature, such as those in [21], where the long tail in the superscaling function is absent. It should be remarked that all of the curves in Fig. 4 essentially satisfy the Coulomb sum rule, i.e., they integrate to unity.

The asymmetry observed in the data has usually been

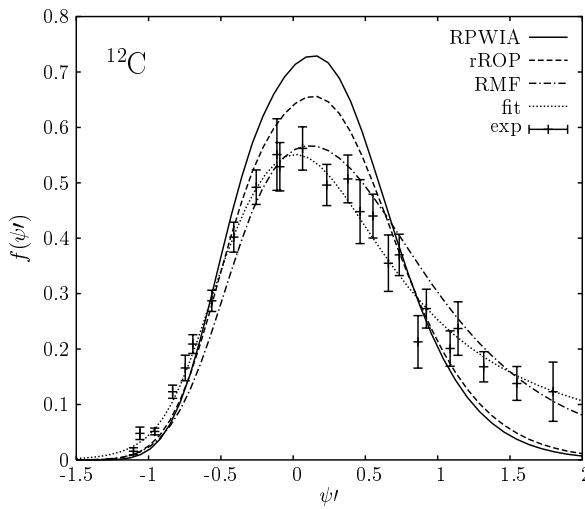


FIG. 4: Scaling function evaluated within the RPWIA (solid), rROP (dashed) and RMF (dot-dashed) approaches compared with the averaged experimental function together with a phenomenological parameterization of the data (dotted).

ascribed to the role played by ingredients beyond the mean field, such as short-range correlations and two-body currents [7]. The results in Fig. 4 appear to reflect the fact that the RMF model includes, or at least mimics,

these types of effects [22]. However, it should be stressed that the main factors responsible for the asymmetry in the calculated scaling function are not only relativity (present in all models considered here), but the particular description of the final continuum nucleon states. The results in Fig. 4 are consistent with the assumption that a universal QE scaling function exists which is valid for inclusive electron and neutrino reactions.

In summary, we have shown that superscaling is fulfilled to high accuracy within the present relativistic impulse approximation in the QE region, and that this holds for the three different descriptions of FSI considered here. The asymmetric shape and the long tail at positive  $\psi'$ -values observed in the experimental scaling function is reproduced only by the RMF model. This result strongly reinforces our confidence in the adequacy of descriptions of FSI effects for inclusive  $(e, e')$  and  $(\nu, \mu)$  reactions when based on the RMF approach.

### Acknowledgements

This work was partially supported by DGI (Spain): BFM2002-03315, BFM2002-03218, FPA2002-04181-C04-04, BFM2003-041-C02-01, by the Junta de Andalucía, and by the INFN-CICYT collaboration agreement N° 04-17. It was also supported in part (TWD) by U.S. Department of Energy under cooperative agreement No. DE-FC02-94ER40818.

---

[1] G. B. West, Phys. Rept. **18**, 263 (1975); D. B. Day, J. S. McCarthy, T. W. Donnelly and I. Sick, Ann. Rev. Nucl. Part. Sci. **40**, 357 (1990).

[2] T.W. Donnelly and I. Sick, Phys. Rev. Lett. **82**, 3212 (1999).

[3] T.W. Donnelly and I. Sick, Phys. Rev. C **60**, 065502 (1999);

[4] C. Maieron, T.W. Donnelly and I. Sick, Phys. Rev. C **65**, 025502 (2002).

[5] L. Alvarez-Ruso, M. B. Barbaro, T. W. Donnelly and A. Molinari, Nucl. Phys. A **724**, 157 (2003); M.B. Barbaro, J.A. Caballero, T.W. Donnelly and C. Maieron, Phys. Rev. C **69**, 035502 (2004).

[6] J. E. Amaro, M. B. Barbaro, J. A. Caballero, T. W. Donnelly and A. Molinari, Nucl. Phys. A **697**, 388 (2002); A **723**, 181 (2003); Phys. Rept. **368**, 317 (2002).

[7] A. De Pace, M. Nardi, W. M. Alberico, T. W. Donnelly and A. Molinari, Nucl. Phys. A **741**, 249 (2004); A. De Pace, M. Nardi, W. M. Alberico, T. W. Donnelly and A. Molinari, Nucl. Phys. A **726**, 303 (2003).

[8] J.E. Amaro, M.B. Barbaro, J.A. Caballero, T.W. Donnelly, A. Molinari and I. Sick, Phys. Rev. C **71**, 015501 (2005).

[9] M. B. Barbaro, R. Cenni, A. De Pace, T. W. Donnelly and A. Molinari, Nucl. Phys. A **643**, 137 (1998).

[10] W. M. Alberico *et al.*, Nucl. Phys. A **623**, 471 (1997).

[11] J.M. Udías *et al.*, Phys. Rev. C **48**, 2731 (1993); **51**, 3246 (1995); **64**, 024614-1 (2001).

[12] W. M. Alberico *et al.*, Phys. Lett. B **438**, 9 (1998); Nucl. Phys. A **651**, 277 (1999).

[13] C. Maieron, M.C. Martínez, J.A. Caballero and J.M. Udías, Phys. Rev. C **68**, 048501 (2003).

[14] C.J. Horowitz and B.D. Serot, Nucl. Phys. A **368**, 503 (1981); Phys. Lett. B **86**, 146 (1979); B.D. Serot and J.D. Walecka, Adv. Nucl. Phys. **16**, 1 (1986).

[15] E.D. Cooper, S. Hama, B.C. Clark and R.L. Mercer, Phys. Rev. C **47**, 297 (1993).

[16] J. Engel, Phys. Rev. C **57**, 2004 (1998); C. Giusti and F.D. Pacati, Nucl. Phys. **A473**, 717 (1987).

[17] G. Co', C. Bleve, I. De Mitri and D. Martello, Nucl. Phys. Proc. Suppl. **112**, 210 (2002) and refs. therein.

[18] C. Bleve *et al.*, Astropart. Phys. **16**, 145 (2001); J. Nieves, J.E. Amaro and M. Valverde, Phys. Rev. C **70** 055503 (2004).

[19] M.M. Sharma, M.A. Nagarajan and P. Ring, Phys. Lett. B **312**, 377 (1993).

[20] J. Jourdan, Nucl. Phys. A **603**, 117 (1996).

[21] J.E. Amaro, M.B. Barbaro, J.A. Caballero, T.W. Donnelly and C. Maieron, ref. nucl-th/0503062 (2005). A. N. Antonov, M. K. Gaidarov, D. N. Kadrev, M. V. Ivanov, E. Moya de Guerra and J. M. Udias, Phys. Rev. C **69**, 044321 (2004); C **71**, 014317 (2005).

[22] J.M. Udías, P. Sarriuguren, E. Moya de Guerra and J.A. Caballero, Phys. Rev. C **53**, R1488 (1996).